Supporting Information

Catalytic Upgrading of Ethanol to Higher Alcohols over Nickel-Modified Cu-La_2O_3/Al_2O_3 Catalysts

Jinfeng He,[a] Xiuzhen Li,[b] Jianyao Kou,[a] Tingjie Tao,[a] Xinyue Shen,[a] Dahao Jiang,[a] Lili Lin[a] and Xiaonian Li[a]*

a. Institute of Industrial Catalysis, Zhejiang University of Technology, Hangzhou 310014, China

b. Fujian Runhua Chemical Co., Ltd., Nanping 354003, China

E-mail addresses: dhjiang@zjut.edu.cn (D.H. Jiang).

Table of Contents

1. Guerbet reaction pathway

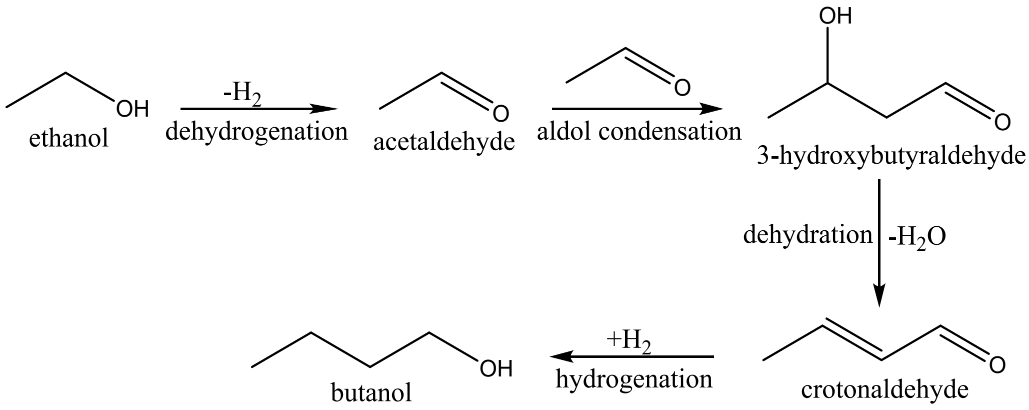

Scheme S1. The Guerbet reaction pathway.

2. Fig. S1. FTIR spectra of CuO/Al_2O_3 catalysts with different CuO loadings

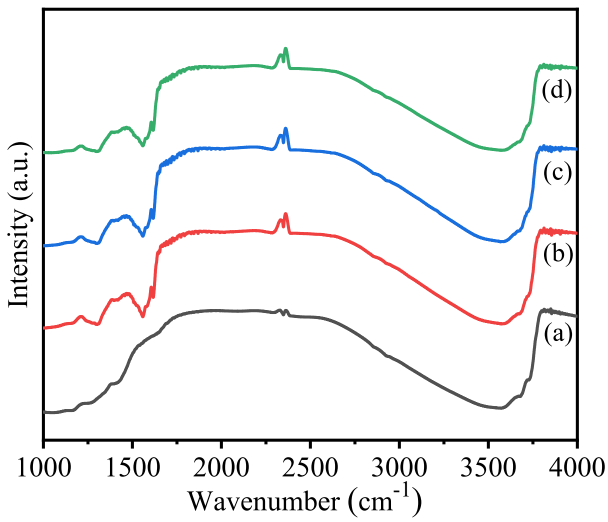

Fig. S1. FTIR spectra of CuO/Al_2O_3 catalysts with different CuO loadings: (a) Al_2O_3; (b) 0.63%CuO/Al_2O_3; (c) 1.25%CuO/Al_2O_3; (d) 1.88%CuO/Al_2O_3.

3. Fig. S2. FTIR spectra of NiO/Al_2O_3 catalysts with different NiO loadings

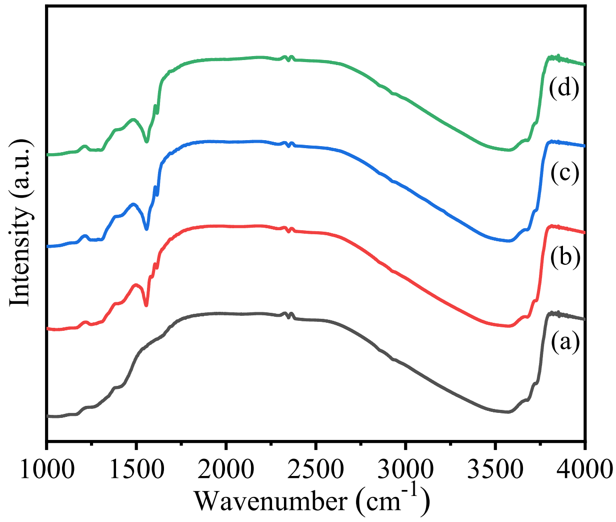

Fig. S2. FTIR spectra of NiO/Al_2O_3 catalysts with different NiO loadings: (a) Al_2O_3; (b) 0.65%NiO/Al_2O_3; (c) 1.27%NiO/Al_2O_3; (d) 1.91%NiO/Al_2O_3.

4. Fig. S3. FTIR spectra of NiO-CuO/Al_2O_3 catalysts with different NiO and CuO loadings

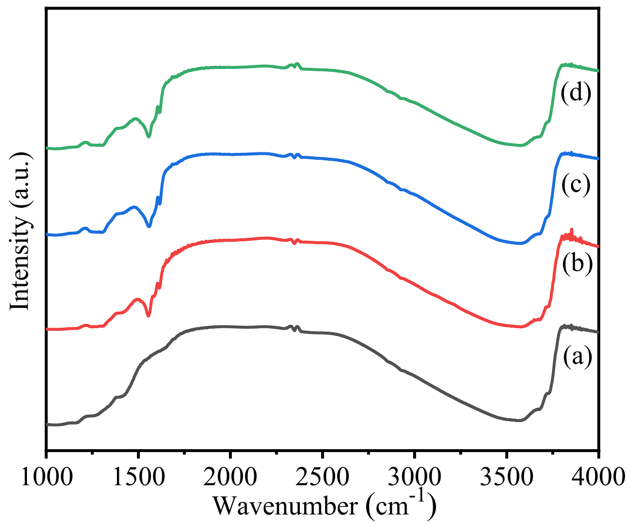

Fig. S3. FTIR spectra of NiO-CuO/Al_2O_3 catalysts with different NiO and CuO loadings: (a) Al_2O_3; (b) 0.32%NiO-0.31%Cu/Al_2O_3; (c) 0.65%NiO-0.63%Cu/Al_2O_3; (d) 0.97%NiO-0.94%Cu/Al_2O_3.

5. Table S1. The areas of -OH absorption peaks for CuO/Al_2O_3 catalysts with different CuO loadings.

Table S1 The areas of -OH absorption peaks centered at 3600 cm^{-1} for Al_2O_3 support and the CuO/Al_2O_3 catalysts with different CuO loadings.

Integral area of IR absorption peak of -OH			
Al_2O_3	0.63%CuO/Al_2O_3	1.25%CuO/Al_2O_3	1.88%CuO/Al_2O_3
63249	63207	63184	51506

6. Table S2. The areas of -OH absorption peaks for NiO/Al_2O_3 catalysts with different NiO loadings.

Table S2 The areas of -OH absorption peaks centered at 3600 cm^{-1} for Al_2O_3 support and the NiO/Al_2O_3 catalysts with different NiO loadings[a].

Integral area of IR absorption peak of -OH			
Al_2O_3	0.65%NiO/Al_2O_3	1.27%NiO/Al_2O_3	1.91%NiO/Al_2O_3
63249	63077	63008	54734

[a] The mass fractions of nickel in the NiO/Al_2O_3 catalysts are respectively equal to those of copper in the corresponding CuO/Al_2O_3 catalysts in Table S1.

7. Table S3. The areas of -OH absorption peaks for $NiO\text{-}CuO/Al_2O_3$ catalysts with different NiO and CuO loadings.

Table S3 The areas of -OH absorption peaks centered at 3600 cm^{-1} for Al_2O_3 support and the $NiO\text{-}CuO/Al_2O_3$ catalysts with different NiO and CuO loadings[a].

Integral area of IR absorption peak of -OH			
Al_2O_3	0.32%NiO-0.31%CuO/Al_2O_3	0.65%NiO-0.63%CuO/Al_2O_3	0.97%NiO-0.94%CuO/Al_2O_3
63249	63373	62808	53550

[a] The mass fractions of nickel and copper are remained to be equal in each $NiO\text{-}CuO/Al_2O_3$ catalyst.

FTIR studies were performed on ThermoFisher Nicolet IS50 instrument (OMNIC software, MCT detector, 64 scans). All catalysts were pressed into 20 mg of self-supporting wafers and mounted into a quartz IR cell with BaF_2 windows. After the catalysts were pretreated at 473 K for 1 h and cooled to desired temperature in a flow of He, FTIR spectra were collected.

FTIR spectra of Al_2O_3 support, CuO/Al_2O_3, NiO/Al_2O_3 and $CuO\text{-}NiO/Al_2O_3$ catalysts with different CuO and/or NiO loadings were shown in Fig. S1-S3† and the areas of -OH absorption peaks centered at 3600 cm^{-1} for the catalysts and Al_2O_3 support were displayed in Table S1-S3†. It can be seen that the intensity of the broad adsorption peak centered at 3600 cm^{-1} characteristic of stretching vibrations of -OH on surface of the catalysts with different CuO loadings first remained almost unchanged and then decreased when the CuO loading gradually increased from 0 to 1.88%.[1,2] The intensity of the broad adsorption peak characteristic of stretching vibrations of -OH on surface of the catalysts with different NiO loadings showed a similar trend when the NiO loading increased from 0 to 1.91%. These results showed that both CuO and NiO preferentially bonded with the surface coordinatively unsaturated Al^{3+} and then bonded with the -OH on the surface of Al_2O_3 support.[3-5]

8. Fig. S4. H_2-TPR profiles of calcined NiO/Al_2O_3 and $NiO\text{-}La_2O_3/Al_2O_3$ catalysts

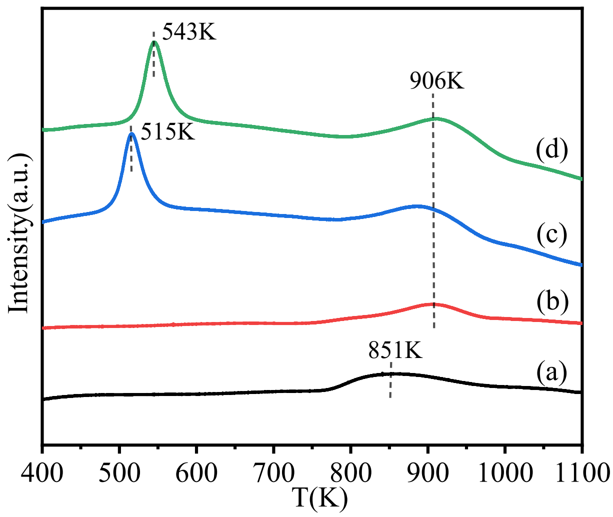

Fig. S4. H_2-TPR profiles of calcined catalysts: (a) 2.55%NiO/Al_2O_3; (b) 2.55%$NiO\text{-}La_2O_3/Al_2O_3$; (c) $Cu\text{-}La_2O_3/Al_2O_3$; (d) 2.55$NiO\text{-}Cu\text{-}La_2O_3/Al_2O_3$.

9. Fig. S5. La 3d XPS spectra of 0.65%NiO-Cu-La_2O_3/Al_2O_3 catalyst after reaction

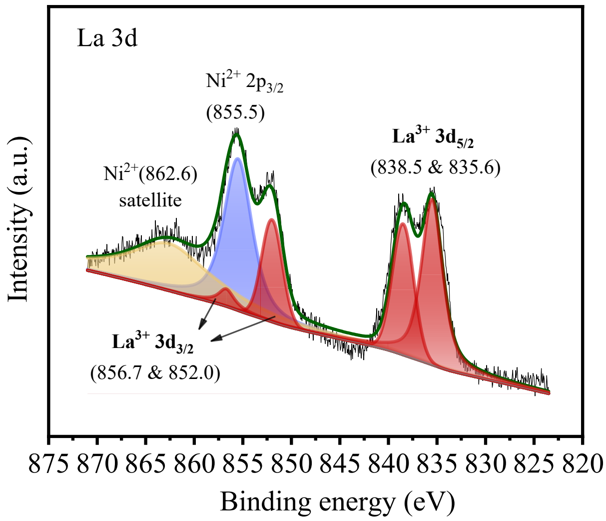

Fig. S5. La 3d XPS spectra of 0.65%NiO-Cu-La_2O_3/Al_2O_3 catalyst after reaction.

10.Table S4. XPS analysis of Cu-La_2O_3/Al_2O_3 and 0.65%NiO-Cu-La_2O_3/Al_2O_3 catalysts

Table S4 XPS parameters of Cu-La_2O_3/Al_2O_3 and 0.65%NiO-Cu-La_2O_3/Al_2O_3 catalysts

Catalyst	Cu 2p (eV)				Ni 2p (eV)		La 3d (eV)				O 1s (eV)	Al 2p (eV)
	$2p_{1/2}$		$2p_{3/2}$		$2p_{1/2}$	$2p_{3/2}$	$3d_{3/2}$		$3d_{5/2}$			
Cu-La_2O_3/Al_2O_3	953.4	952.3	933.4	932.1	—	—	856.8	852.1	838.4	835.6	531.1	73.9
0.65%NiO-Cu-La_2O_3/Al_2O_3	953.7	952.5	933.6	932.3	873.8	855.5	856.7	852.0	838.5	835.6	531.0	74.0

11. Table S5. Textural parameters and surface properties of NiO-Cu-La_2O_3/Al_2O_3 catalysts

Table S5 Textural parameters and surface properties of NiO-Cu-La_2O_3/Al_2O_3 catalysts.

Catalyst[a]	S_{BET} (m^2/g)	V_t[b] (cm^3/g)	D_{pore}[c] (nm)	Total acidity ($mmol\cdot g^{-1}$)	Acidity distribution ($mmol\cdot g^{-1}$)			Total basicity ($mmol\cdot g^{-1}$)	Basicity distribution ($mmol\cdot g^{-1}$)		
					Weak	medium	strong		Weak	medium	strong
Cu-La_2O_3/Al_2O_3	155.7	0.53	12.7	1.65	1.13	0.41	0.11	0.72	0.12	0.11	0.49
0.32%NiO-Cu-La_2O_3/Al_2O_3	167.4	0.57	12.9	1.48	0.99	0.39	0.10	0.77	0.12	0.12	0.53
0.65%NiO-Cu-La_2O_3/Al_2O_3	173.6	0.57	12.4	1.33	0.95	0.31	0.07	0.84	0.13	0.10	0.61
1.27%NiO-Cu-La_2O_3/Al_2O_3	166.6	0.57	12.9	—	—	—	—	—	—	—	—
2.55%NiO-Cu-La_2O_3/Al_2O_3	165.5	0.56	12.9	1.38	0.92	0.40	0.06	0.78	0.14	0.12	0.52

[a] The Cu loadings of all the catalysts were fixed at 6wt% and the Cu/La molar ratios were 3:1.5; [b] Single point pore volume at P/P_0=0.99; [c] The average pore diameters (DFT method).

12. Fig. S6. Stability evaluation of 0.65%NiO-Cu-La_2O_3/Al_2O_3 catalyst

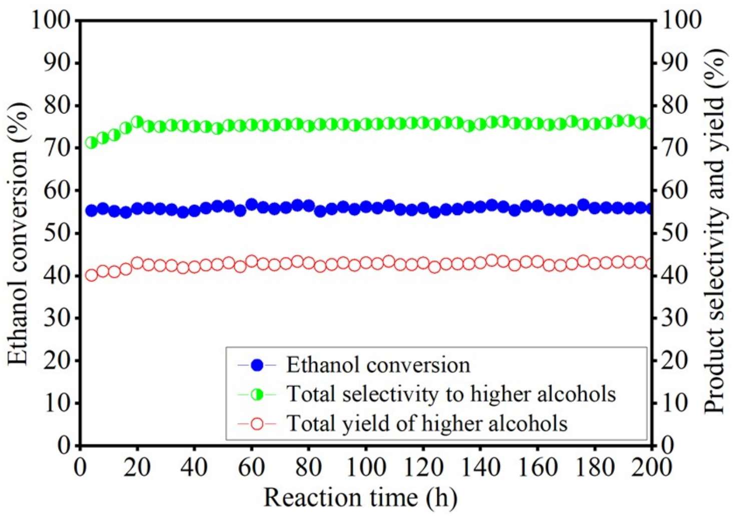

Fig. S6. Stability evaluation of 0.65%NiO-Cu-La_2O_3/Al_2O_3 catalyst.

13. Table S6. Catalytic performance of NiO/Al_2O_3 and $NiO-La_2O_3/Al_2O_3$ catalysts for upgrading ethanol to higher alcohols

Table S6. Catalytic performance of NiO/Al_2O_3 and $NiO-La_2O_3/Al_2O_3$ catalysts for ethanol upgrading to higher alcohols[a]

Catalysts	Conversion (%)	Selectivity (%)		Liquid yield (%)
		Ethyl ether	Others[b]	
0.65%NiO/Al_2O_3	12.5	100	0	99.5
0.65%$NiO-La_2O_3/Al_2O_3$	4.6	100	0	99.4

[a] Conversion and selectivity are obtained at steady-state; reaction conditions: catalyst, 1.0 g; 523 K, 3 MPa (N_2), LHSV=2 ml/(g_{cat}·h), N_2/ethanol(v/v)=250:1. [b]Other products include acetaldehyde, butyraldehyde, ethyl acetate, n-butanol, etc.

References

1. M. I. Zaki and H. Knözinger, *Mater. Chem. Phys.*, 1987, **17**, 201-215.
2. F. Wang, J. Z. Ma, S. H. Xin, Q. Wang, J. Xu, C. B. Zhang, H. He and X. C. Zeng, *Nat. Commun.*, 2020, **11**, 529.
3. E. Borello, A. Cimino, G. Ghiotti, M. Lo Jacono, M. Schiavello and A. Zecchina, *Discuss. Faraday Soc.*, 1971, **52**, 149-160.
4. C. Zhao, Y. Z. Yu, A. Jentys and J. A. Lercher, *Appl. Catal., B*, 2013, **132**, 282-292.
5. Y. M. Zhang, Y. Zu, D. D. He, J. Liang, L. H. Zhu, Y. Mei and Y. M. Luo, *Appl. Catal., B*, 2022, **315**, 121539.